Intrinsic stress, island coalescence, and surface roughness during the growth of polycrystalline films

Brian W. Sheldon, K. H. A. Lau, and Ashok Rajamani

Citation: Journal of Applied Physics **90**, 5097 (2001); doi: 10.1063/1.1412577
View online: http://dx.doi.org/10.1063/1.1412577
View Table of Contents: http://scitation.aip.org/content/aip/journal/jap/90/10?ver=pdfcov
Published by the AIP Publishing

Intrinsic stress, island coalescence, and surface roughness during the growth of polycrystalline films

Brian W. Sheldon,[a] K. H. A. Lau, and Ashok Rajamani
Division of Engineering, Brown University, Providence, Rhode Island 02912

(Received 5 February 2001; accepted for publication 21 August 2001)

During film growth by a variety of techniques, intrinsic tensile stresses can be created by the coalescence of neighboring islands. Experimental results with diamond films produced by chemical vapor deposition are compared with a relatively simple model to demonstrate that a realistic interpretation of these coalescence stresses must account for effects that are associated with surface roughness. First, the interpretation of curvature measurements during the early stages of film growth must account for this surface roughness. Also, the experiments show that tensile stresses are induced by grain boundary formation during continuing growth after the initial island coalescence event. This understanding differs from the traditional interpretation that continuing intrinsic stress is produced by ''templated'' growth onto an already strained crystalline lattice. A kinetic model of stress evolution during postcoalescence growth is also presented. © *2001 American Institute of Physics.* [DOI: 10.1063/1.1412577]

I. INTRODUCTION

Stress created during the deposition of thin films and coatings can be a major factor in the performance and failure of many of these materials. Residual thermal stresses can be readily calculated if values for the thermal expansion coefficients are known. However, intrinsic stresses, which are created by the growth process, are often more difficult to assess and control. In many polycrystalline materials, it has long been suspected that a major source of residual tensile stress is the formation of grain boundaries during the coalescence of individually nucleated clusters.[1–3] These mechanisms were first considered by Hoffman.[1,2] Pioneering studies by Abermann and Koch have explored these stresses in more detail, primarily in metals.[4,5]

Hoffman originally estimated the tensile stress resulting from crystallite coalescence as

$$\sigma = M_f \frac{\delta}{L}, \tag{1}$$

where M_f is the biaxial modulus of the film (i.e., $E/(1-\nu)$), L is the grain size, and δ is the gap between neighboring crystals. This expression is based on the premise that grains that are separated by a distance δ can ''pull together'' to form a grain boundary. The value of δ is typically viewed as an atomic-scale distance. This coalescence process gives rise to tensile stress, driven by the reduction in interfacial/surface energies, described by

$$\Delta\gamma = \gamma_I - 2\gamma_S, \tag{2}$$

where γ_I is the free energy of the newly formed grain boundary, and γ_S is the free energy of the solid/vapor surfaces prior to coalescence (note that $\Delta\gamma$ must be negative for coalescence to be thermodynamically viable).

We previously obtained a relatively simple expression for the biaxial stress which depends on $\Delta\gamma$, instead of δ:[6,7]

$$\sigma_{\mathrm{MAX}} = \left[\frac{-2M_f\Delta\gamma}{L}\right]^{1/2}. \tag{3}$$

This equation is based on a square lattice of grains which impinge simultaneously to form a film with a flat top surface. The value obtained from Eq. (3) is an upper bound because it assumes that all of the energy reduction associated with $\Delta\gamma$ is converted to elastic strain, and because it ignores all relaxation mechanisms that might act to reduce the stress.

Nix and Clemens independently obtained Eq. (3) for a hexagonal array of grains, also noting that this is an upper bound.[8] This work by Nix and Clemens also presents a more detailed treatment where the coalescence of two-dimensional (2D) elliptical islands is viewed as a reverse crack growth process. This results in an expression for the stress in the lower, continuous portion of the film that is similar to Eq. (3). Recently Freund and Chason have presented a more general treatment of initial coalescence based on contact mechanics, which results in the following expression:[9]

$$\frac{\sigma_V}{E} = A_N\left[\frac{-\Delta\gamma}{EL}\right]^{C_N}, \tag{4}$$

where σ_v is the volume averaged stress, and A_N and C_N are constants that depend on the dimensionality of the problem. In terms of Eq. (4), the derivation of Eq. (3) corresponds to one dimensional contact surfaces where $C_I = \frac{1}{2}$.[9]

Both Eqs. (3) and (4) are based on the premise that all of the tensile coalescence stress evolves at the point where neighboring islands impinge on each other. Additional mechanisms such as grain growth or dislocation formation

[a]Author to whom correspondence should be addressed; electronic mail: brian_sheldon@brown.edu

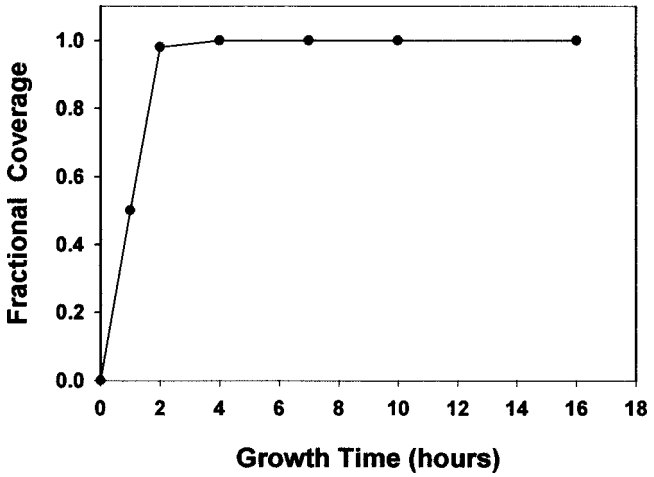

FIG. 1. Surface coverage vs time (based on SEM images).

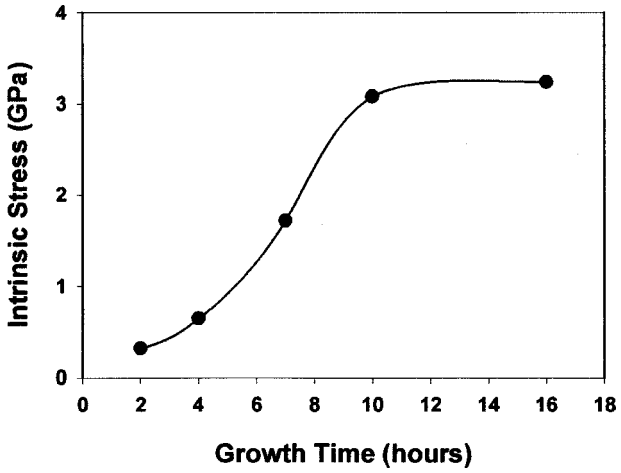

FIG. 2. Stress based on curvature measurements and Eq. (5).

could alter the growth stress as deposition proceeds past the initial coalescence point. In the absence of additional mechanisms, previous researchers have speculated that subsequent epitaxial film growth on these crystals should maintain the tensile stress created by island coalescence, because additional atomic layers will be templated onto the underlying stressed crystalline lattice.[2,8] In this simplified case, the tensile stress is fully evolved at the ''coalescence point'' where the substrate surface is first completely covered by the film, and then remains unchanged during further growth. This understanding appears to be flawed, based on the experimental and modeling results that are presented below.

II. EXPERIMENTS WITH CHEMICAL VAPOR DEPOSITED DIAMOND

Polycrystalline diamond formed by chemical vapor deposition (CVD) has a number of features which make it an attractive system for conducting basic investigations of coalescence stress. Previous researchers have reported large intrinsic tensile stresses in CVD diamond that have generally been attributed to island coalescence.[10–13] There are other mechanisms besides island coalescence that can induce intrinsic tensile stress in a thin film, however, the low atomic mobilities in diamond minimize most of these effects. For example, grain growth is essentially nonexistent during the growth of CVD diamond, and is thus not expected to contribute to the observed tensile stress. Also, surface and grain boundary diffusion in diamond are believed to be very slow, such that these mechanisms are unlikely to produce significant stress relaxation. The stresses observed in diamond are also not consistent with the densification of an amorphous grain boundary phase, particularly since a substantial grain boundary phase in these films has not been observed by transmission electron microscopy.[14]

Diamond films on (001) Si substrates were grown by CVD at 800 °C, 38 Torr, and 1% CH_4 in a hydrogen plasma (AsTex HPM/M microwave-plasma reactor operating at 1200 W). A detailed description of the procedures used to prepare and characterize these films was presented previously.[7,13] Plots of surface coverage and intrinsic stress versus deposition time are presented in Figs. 1 and 2. Scanning electron microscope (SEM) images were used to obtain the surface coverages reported in Fig. 1, the film thickness (see Sec. III B), and approximate grain sizes (1–2 μm). These measurements were all consistent with other films grown under similar conditions.[13] Stresses were determined by measuring curvature with laser-deflection. The traditional method of converting curvature R to stress σ uses Stoney's equation when the film thickness is negligible compared to the substrate thickness. The diamond film thicknesses are close to this limiting case, however, it is more appropriate to use a modified form of Stoney's equation[15]

$$\sigma = \frac{M_S H_S^2}{6RH_f}\left[1 + 4\frac{M_f H_f}{M_S H_S} - \frac{H_f}{H_S}\right], \tag{5}$$

where M_S, H_S, M_f, and H_f are the biaxial moduli and thicknesses of the substrate and film, respectively. It is important to note that the derivation of Eq. (5) is based on a film with a uniform thickness (i.e., negligible surface roughness). The stresses determined with Eq. (5) were corrected for the thermal stress induced during cooling to give intrinsic growth stresses; these values are plotted in Fig. 2. These thermal corrections were also verified by making curvature measurements at elevated temperatures, in films that were reheated following deposition.

In some cases, there can be significant plastic deformation of the Si substrate during diamond film growth.[11,16] This is problematic because it invalidates Eq. (5), which is based on an elastic substrate. To investigate this possibility, several films grown for at least 10 h were annealed for an additional 12 h at the growth temperature. This consistently produced less than a 2% change in the radius of curvature, thus indicating that inelastic deformation of the substrate has little or no effect on the reported stress values. Similar anneals at 900 °C also failed to produce any significant change in the measured curvature. Note that the highest stresses in the substrate occur near the substrate/film interface, thus localized substrate plasticity could influence stress evolution mechanisms during film growth, even though this does not have a significant effect on the curvature measurements.[17]

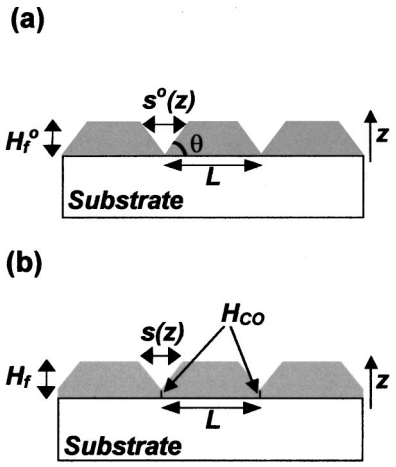

FIG. 3. Schematic of the island coalescence mechanism: (a) undeformed islands at the point where they first impinge (i.e., at $t=t_C$); (b) deformed islands immediately after the initial onset of intrinsic stress due to grain boundary formation (i.e., at $t=t_C$).

Based on the results in Fig. 1 the films grown under these conditions are completely coalesced at 2–3 h. At this point the tensile stresses according to Eq. (5) are only a fraction of the maximum value observed at longer growth times. Similar behavior has also been observed elsewhere.[12,13] The data in Figs. 1 and 2 show that the intrinsic tensile stress increases at a relatively rapid rate following complete coalescence. Based on these data and previously reported results,[13] the intrinsic stress asymptotically approaches a relatively constant value after a much longer time. In contrast to this observation, the analyses leading to Eqs. (3) and (4) do not predict time-dependent stress evolution. Some discrepancy occurs because Eqs. (3) and (4) are based on an ordered array of islands which nucleate simultaneously, such that all of the islands coalesce at the same time. Island nucleation is typically random, both spatially and temporally. This creates a distribution of island separations and island sizes, such that coalescence is not instantaneous, but instead occurs during a certain range of times. This distribution can explain a gradual evolution of stress, similar to the general shape of the curve in Fig. 1. However, this range of coalescence times does not account for the increasing stress that is observed a long time after the islands coalesce into a continuous film.

III. MODEL

A. Stress at coalescence

The schematics in Fig. 3 illustrate the formation of intrinsic stress at the point where neighboring islands first impinge. Each island is assumed to be stress free before it grows into its neighbors. Although not strictly valid, this is a reasonable assumption because precoalescence stresses should be much smaller than the observed postcoalescence tensile stresses. A recent analysis predicts that the Laplace pressure due to surface curvature creates stresses in small, isolated islands.[18] Surface tensions are usually positive, so these stresses are usually compressive, with a magnitude on the order of $2\ \gamma_S/L$. This corresponds to less than 10 MPa for $\sim 1\ \mu$m diamond islands immediately before they impinge on their neighbors (although Cammarata *et al.* suggest that larger stresses could be ''locked in'' before the islands reach this size).[18] Our curvature measurements are also consistent with small stresses prior to coalescence (i.e., before a growth time of 2 h in Fig. 2).

Diamond crystals grow with a cubo-octahedral shape, however, the shape in Fig. 3(a) is more amenable to the relatively simple analysis presented here. This shape can be interpreted as {001} facets on the top surface, and diagonal facets whose Miller indices depend on the angle. This geometry has also been used by Tersoff and co-workers to describe isolated, strained semiconductor islands.[19] The analysis used to obtain Eq. (3) is based on a three-dimensional version of the configuration in Fig. 3, for the limiting case where $\theta=\pi/2$. When the islands depicted in Fig. 3 exist with $\theta<\pi/2$, growth past coalescence produces a nonplanar surface, such that the film can be viewed as a lower, continuous section and an upper, rough section. The model presented in this section is thus an extension of the analyses that lead to Eq. (3), for the more general case where θ can have a range of different values.

In our analysis all islands nucleate simultaneously with a periodic separation L, such that they all impinge at the same time t_C. While not physically realistic, this approach makes it possible to isolate the effects of stress evolution during island coalescence without considering the far more complicated stress fields that will be caused by a distribution of island positions and nucleation times. With the configuration in Fig. 3, islands with the same orientation are still assumed to form a grain boundary when they impinge. This makes it possible to analyze boundary formation without the additional complexities caused by variations in grain alignments. The diamond crystals described in Sec. II are highly misoriented, however, the model presented here more closely resembles the impingement of aligned epitaxial islands (note that epitaxial islands can still form grain or domain boundaries because of small misalignments).

For the formulation presented here, surface and grain boundary diffusion are assumed to be negligible. Island growth and impingement in the absence of any stress effects are considered first. The kinetics of this process are dictated by two growth velocities, u_T and u_E, which correspond to the top surfaces and edges, respectively. The coalescence time is then given by

$$t_C=\frac{L}{2u_E\sin\theta}, \tag{6}$$

where L is the dimension of the base of the island (and thus also the separation between island centers). The unstrained island height at coalescence is given by

$$H_f^o(t_C)=u_T t_C. \tag{7}$$

By analogy with Eqs. (3) and (4), the following expression is used to approximate the average, coalescence stress along the grain boundary at the time that coalescence first occurs:

$$\langle \sigma \rangle = AE\left[\frac{-\Delta\gamma}{EL}\right]^C. \tag{8}$$

This stress is uniaxial for 2D islands or biaxial for 3D islands, where the brackets $\langle\ \rangle$ follow the notation in Ref. 8. Finite element modeling (FEM) can be used to obtain values for the constants in Eq. (8). In general, this shows that A and C vary with θ and with the island dimensionality.[20] It is important to recognize that Eq. (8) is an approximation that provides a relatively simple and reasonable basis for the model development in the rest of this section. Note that an alternative expression for $\langle\sigma\rangle$ could be substituted into the derivations which follow, without changing the two basic conclusions that are listed at the end of Sec. IV.

When the surface roughness is a small fraction of the total film thickness, $\langle\sigma\rangle$ approaches σ_{MAX}. Thus Fig. 2 suggest a σ_{MAX} value of roughly 3.3 GPa. With the measured values of L, this value of σ_{MAX} corresponds to $\Delta\gamma \sim 1-4$ J/m^2 based on Eq. (8). This is roughly consistent with estimated values for diamond growth surfaces and grain boundaries.[21–23]

For the geometry in Fig. 3, the average coalescence-induced strain along the grain boundary can be estimated as

$$\langle \epsilon \rangle = \frac{1}{H_{\mathrm{CO}}}\int_0^{H_{\mathrm{CO}}} \epsilon(z)\,dz = \frac{1}{H_{\mathrm{CO}}}\int_0^{H_{\mathrm{CO}}} \frac{2z\cot\theta}{L}\,dz$$

$$= \frac{H_{\mathrm{CO}}}{L}\cot\theta. \tag{9}$$

The function $\epsilon(z)$ is the average uniaxial or biaxial strain in the film at some height z. This average is taken parallel to the substrate surface, as opposed to the brackets $\langle\ \rangle$ which again denote the average of $\epsilon(z)$ taken in the z direction. The average stress and strain can be related by the elastic properties of the film $\langle\sigma\rangle = M_f\langle\epsilon\rangle$. Combining this with Eqs. (8) and (9) and rearranging gives the following expression for the grain boundary height at t_C:

$$H_{\mathrm{CO}} = AL\,\frac{E}{M_f}\tan\theta\left[\frac{-\Delta\gamma}{EL}\right]^C. \tag{10}$$

Note that the total in-plane force acting along the boundary height should be equal to the total in-plane force acting along the middle of the grain (i.e., from $z=0$ to $z=H_f$). This implies that the average stress along the boundary $\langle\sigma\rangle$ is significantly larger than the average stress in the middle of the grain. This was verified with finite element calculations.[20]

B. Film thickness, surface roughness, and stress

Using Eq. (5) to convert curvature to stress assumes that the film thickness is uniform, however SEM images such as those in Fig. 4 clearly show that this is not the case for polycrystalline diamond. Long after the individual islands coalesce, there is still considerable roughness associated with gaps between the tops of the faceted grains. This roughness is effectively ignored when the measured grain height is interpreted as the film thickness, and then inserted into Eq. (5). To understand the inherent error in this approach, consider

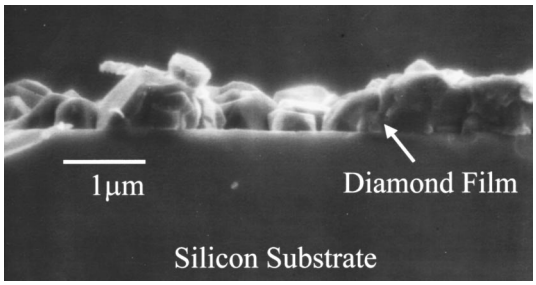

FIG. 4. SEM cross section after 2 h of growth.

the geometry analyzed in the preceding section (see Fig. 3). The stress along the grain boundary is more directly related to the coalescence event, thus the grain boundary height H_C provides a better measure of the film thickness associated with coalescence stresses. Thus the stress values where the asterisk denotes a value that is an effective average over the area of the film. The relationship between H_C^* and the actual film microstructure requires a more detailed model of microstructure evolution and stress. This type of analysis is beyond the scope of the work presented here, however, the value of H_C^* should clearly be less than H_f.

When surface roughness is considered, the data in Fig. 2 can be reinterpreted to produce the results in Fig. 5. In this plot $\langle\sigma\rangle$ is an average stress value along grain boundaries, and σ_{MAX} is the asymptotic limiting value obtained from experiments (i.e., the value for an essentially planar film). Thus the ratio $H_C^*\langle\sigma\rangle/H_f\sigma_{\mathrm{MAX}}$ in Fig. 5 asymptotically approaches 1 as growth proceeds past coalescence and the relative film roughness decreases. At shorter times, the measured curvature reflects the value $H_C^*\langle\sigma\rangle$. If $\langle\sigma\rangle = \sigma_{\mathrm{MAX}}$ (i.e., the stress quickly reaches its limiting value), then H_C^* can be obtained from Eq. (5) by inserting the measured curvature and the value of σ_{MAX}. In this case the only unknown quantity remaining in Eq. (5) is H_f, which can then be reinterpreted as a measured value of H_C^*.

For the general case where $\langle\sigma\rangle$ and σ_{MAX} are not equal, additional information is necessary to deconvolute values of H_C^* and $\langle\sigma\rangle$ from the curvature values. One approach is to try to measure H_C^* values. It is not practical to obtain this aver-

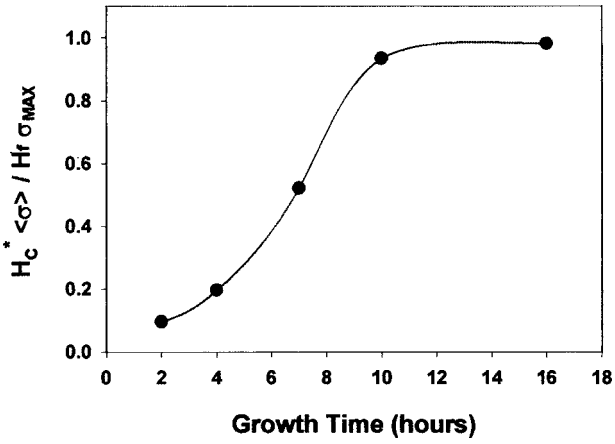

FIG. 5. Plot of H_C^*/H_f based on reassessing the data in Fig. 2 with the assumption that the stress in the continuous part of the film is constant.

age grain boundary height from SEM images. Surface roughness values obtained by atomic force microscopy indicate that the total surface roughness does not change significantly as a function of growth time (for the samples in Fig. 1). At all of the growth times, the rms roughness was 0.1–0.2 μm, with a slight increase observed at longer times. The corresponding film thickness increased from 0.7 μm at 2 h, to 4.8 μm at 16 h. It is difficult to use the rms roughness values as a direct measure of H_C^*. If the difference between H_f and H_C^* is interpreted as roughly twice the rms value, then the continuous portion of the film is ~60%–80% of the film thickness after only 4 h of growth. At this point, the ratio in Fig. 5 is far less than 0.6, which suggests that $\langle\sigma\rangle$ has not yet reached σ_{MAX}. Further study of this behavior is needed, however, this result indicates that the intrinsic tensile stress continues to increase after the initial coalescence event (i.e., after t_C).

At coalescence, Eqs. (6), (7), and (10) can be combined to give the following expression for the initial, relative grain boundary height:

$$\frac{H_C(t_C)}{H_f^O(t_C)} = \frac{AE\sin^2\theta}{M_f\mu\cos\theta}\left[\frac{-\Delta\gamma}{EL}\right]^C, \tag{11}$$

where $\mu = u_T/u_E$. For values that correspond to CVD diamond, Eq. (11) predicts that the initial grain boundary height will be very small compared to the film thickness. It is difficult to verify this experimentally, because the growth process cannot be halted at exactly the point where grains initially coalesce. However, a short initial boundary height is consistent with the idea that most of the coalescence stress evolves after t_C.

The models in Sec. III A, along with those proposed by Hoffman[2] and others,[6–9] do not explicitly consider stress evolution after the initial point where neighboring islands impinge. As already noted, previous researchers have postulated that tensile stress induced by island coalescence is retained because continued homoepitaxial growth is templated onto the existing crystalline lattice.[2,8] This is not consistent with the observation that $\langle\sigma\rangle$ apparently increases after coalescence. It is perhaps even more important to note that the stress state at the tops of these islands should be considerably less tensile than the stress given by Eq. (8).[19,20,24] Thus ''templated'' growth onto the rough diamond surfaces will produce stresses that are considerably lower than the tensile stresses in the underlying continuous portion of the film. This further reinforces the conclusion that ''templating'' cannot explain the experimental observations.

C. Growth on rough surfaces

The growth of a coaleseed film begins at t_C (i.e., the point where islands initially impinge, as seen in Fig. 3). At this time the neighboring edge facets do not coalesce into a grain boundary for $z > H_{\mathrm{CO}}$, because this would produce an average stress in the film which exceeds the energetic limit given by Eq. (8). However, subsequent growth onto these exposed edge facets will reduce the gap between them. When this gap $s(z)$ is small enough, coalescence becomes energetically favorable. At an arbitrary height z, the average strain due to coalescence is estimated as:

$$\epsilon(z) = \frac{s^o(z)}{L}, \tag{12}$$

where $s^o(z)$ is the separation distance between neighboring facets that would occur if growth continued past the initial coalescence point without producing any deformation in the film

$$s^o(z) = 2z\cot\theta - 2u_E\sin\theta(t - t_C). \tag{13}$$

The first term in Eq. (13) is the gap between neighboring edge facets for the undeformed configuration at the coalescence time. The second term accounts for the material deposited by additional growth after t_C. Substituting Eq. (13) into Eq. (12) at the point where $z = H_C$ (the coalesced grain boundary height), and equating this with the maximum allowable stress gives:

$$\epsilon(H_C) = \frac{2}{L}[H_C\cot\theta - u_E\sin\theta(t - t_C)] = \frac{\langle\sigma\rangle}{M_f} = \langle\epsilon\rangle. \tag{14}$$

Combining this with the value of $\langle\sigma\rangle$ specified by Eq. (8) and rearranging gives

$$H_C(t) = \frac{\tan\theta}{1-\langle\epsilon\rangle}\left[u_E\sin\theta(t - t_C) + \frac{L}{2}\langle\epsilon\rangle\right], \tag{15}$$

$$\langle\epsilon\rangle = \frac{AE}{M_f}\left[\frac{-\Delta\gamma}{EL}\right]^C. \tag{16}$$

A convenient dimensionless form of Eq. (15) is

$$h_C(\tau) = \frac{H_C(t)}{(L/2)} = \frac{\tan\theta}{1-\langle\epsilon\rangle}[\sin\theta(\tau - 1) + \langle\epsilon\rangle], \tag{17}$$

$$\tau = \frac{t}{t_C}. \tag{18}$$

This expression is only applicable for $\tau \geqslant 1$ (i.e., after initial coalescence). When the strain is relatively small, this model predicts that the increase in grain boundary height is essentially linear in time. This relatively simple model also assumes that $\epsilon(z) = \langle\epsilon\rangle$ (i.e., constant) during boundary formation after t_C (i.e., for $H_{\mathrm{CO}} \leqslant z \leqslant H_C$). In contrast to this, the treatments of initial coalescence in Sec. III A and in Ref. 8 lead to $\epsilon(z)$ values that vary with z for the initial boundary formation process at $t = t_C$ (i.e., for $z \leqslant H_{\mathrm{CO}}$). This is evident in Eq. (9), where the average strain is $\langle\epsilon\rangle$, but $\epsilon(H_{\mathrm{CO}})$ is equal to $2\langle\epsilon\rangle$. Thus, comparing the model in Sec. III A with Eq. (14) shows a sharp discontinuity in $\epsilon(z)$ at $z = H_{\mathrm{CO}}$. This discontinuity is not expected to occur in a real film, and is addressed in more detail in a subsequent article on our FEM results.[20] This FEM work also shows that stress evolution during continued growth is more complex than the simple model developed here. Fitting these FEM results to Eq. (16) produces values of A and C that vary as the film thickness increases. These differences reflect geometric effects, since the incremental coalescence strain during growth is constant [i.e., an increase in C is accompanied by a decrease in A,

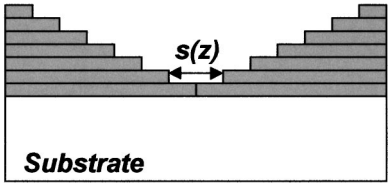

FIG. 6. Schematic of island coalescence during film growth, based on step motion associated with distinct atomic layers.

such that $\epsilon(H_C)$ given by Eq. (14) is constant]. Variations such as this also indicate that the form of Eq. (16) oversimplifies the strain evolution that occurs during growth beyond the coalescence point.

IV. DISCUSSION AND CONCLUSIONS

The model developed in Sec. III A can also be interpreted on an atomic length scale. For example, the edge facets in Fig. 3 can be viewed as a series of atomic layers parallel to the substrate, as shown in Fig. 6. For a layer with mean height $z=z_A$, the separation between the steps on neighboring grains is still given by $s^o(z_A)$ according to Eq. (13). The values for grain boundary height and strain in the continuous portion of the film are then identical to those obtained above for the continuum model. With this layer by layer concept in mind, note that the grain boundary heights and strain in Eqs. (15) and (16) are upper bound estimates. As noted above, there are certain relaxation processes that can reduce the tensile coalescence stress. In the absence of these effects, the process depicted in Fig. 6 can still produce less stress than the energetic limit defined by Eq. (8). To achieve this maximum value, the atomic layers in neighboring grains must pull together as soon as it is thermodynamically favorable [i.e., as soon as Eq. (8) is satisfied]. However, if the two steps are far enough apart, the forces between the atoms at these steps will be too weak to cause coalescence. In this case, growth will proceed until these attractive forces can act. This will lead to lower coalescence strains than the predictions in Eq. (16). The corresponding value of H_C will also be less than that given by Eq. (15).

The simple geometry used in Sec. III is clearly oversimplified compared to real polycrystalline films. A more precise description would include the effects of grain size distributions, grain orientations, and the eventual evolution of columnar grains (which has not yet occurred in the diamond films described in Sec. II). More realistic random microstructures are readily described with conventional mean field approaches (e.g., Avrami models), however, the complex grain geometry in a real film makes it is much more difficult to properly analyze stress distributions during film growth. In particular, the spatial and temporal randomness of nucleation during the deposition of a real film means that coalescence will not mimic the symmetric geometries used here and in Refs. 6 and 8. In more realistic random microstructures, the simple biaxial stress approximation is no longer reasonable, and a full tensor representation of the mechanics is required. Recently, Seel *et al.* used a computer simulation to explore stress evolution in random microstructures.[25] They predict that periodic models can overpredict coalescence stresses. However, their model only produces coalescence stress at the initial time (i.e., at t_C). Our results show that most coalescence stress evolves after the initial impingement, which suggests that the periodic model in Sec. III C will not overpredict stress to the same degree. Verification of this supposition requires additional computational work.

Our previous experimental results show that variations in the growth chemistry can be used to vary stress evolution during postcoalescence growth.[14] These observations are consistent with the idea that boundary formation after the initial coalescence event continues to produce tensile stress in the film. In contrast, these observations are not readily explained by earlier models (i.e., if the tensile stress generated at the coalescence point was templated onto strained crystals). Thus, the model presented here has important implications because it demonstrates that the deposition process can be regulated to control intrinsic stresses and stress gradients during film growth in a way which is independent of grain size and grain size distribution effects.

The model developed in Sec. III is a starting point for understanding how intrinsic tensile stress continues to evolve during film growth beyond the initial coalescence event. It provides important insight into two experimentally observed phenomena. These can be summarized as follows:

(1) When curvature measurements are converted to stress with Eq. (5) (or with Stoney's equation), the results can be misleading because surface roughness effects are ignored. The actual tensile stresses in the vicinity of the grain boundary should be much larger than those elsewhere. An estimate of the stress along the grain boundary can be obtained with Eq. (5), if the film thickness H_f is replaced with an effective grain boundary height H_C^*.

(2) As growth proceeds past the initial coalescence point, the lower strains in the upper portion of the film invalidate the idea that a constant stress is maintained by templated growth on an already strained surface. Instead, the model in Sec. III C predicts that grain boundary formation during growth continues to generate intrinsic stress, well beyond the point where isolated islands first coalesce.

ACKNOWLEDGMENTS

This research was supported by the National Science Foundation, under Award Nos. DMR-9619520 and DMR-0075207. This work also made use of MRSEC Shared Experimental Facilities supported by the National Science Foundation under Award No. DMR-963254. The authors are also grateful to Professor Allan Bower, Professor Eric Chason, Professor Ben Freund, and Professor Janet Rankin for their insights and suggestions regarding this work.

[1] J. D. Finegan and R. W. Hoffman, J. Appl. Phys. **30**, 587 (1959).
[2] F. A. Doljack and R. W. Hoffman, Thin Solid Films **12**, 71 (1972).
[3] M. Doerner and W. D. Nix, CRC Crit. Rev. Solid State Mater. Sci. **14**, 225 (1986).
[4] R. Abermann and R. Koch, Thin Solid Films **129**, 71 (1985).
[5] R. Koch and R. Abermann, Thin Solid Films **140**, 217 (1986).
[6] S. Nijhawan, J. Rankin, B. L. Walden, and B. W. Sheldon, in *MRS Symposium Proceedings*, 1997, edited by R. Cammarata *et al.* (Materials Research Society, Pittsburgh, PA, 1998), Vol. 505, p. 415.
[7] S. Nijhawan, Ph.D. thesis, Brown University, 1998.

[8] W. D. Nix and B. M. Clemens, J. Mater. Res. **14**, 3467 (1999).
[9] L. B. Freund and E. Chason, J. Appl. Phys. **89**, 4866 (2001).
[10] H. Windischmann, G. F. Epps, Y. Cong, and R. W. Collins, J. Appl. Phys. **69**, 2231 (1991).
[11] L. Schafer, X. Jiang, and C. Klages, in *Applications of Diamond and Related Materials*, edited by Y. Tzeng *et al.* (Elsevier, New York, 1991), p. 121.
[12] D. Schwartzbach, R. Haubner, and B. Lux, Diamond Relat. Mater. **3**, 757 (1994).
[13] S. Nijhawan, S. M. Jankovsky, B. W. Sheldon, and B. L. Walden, J. Mater. Res. **14**, 1046 (1999).
[14] B. W. Sheldon, S. Nijhawan, J. Rankin, and B. L. Walden, in *Proceedings of the 6th Symposium on Diamond Material*, edited by J. C. Angus *et al.* (Electrochemical Society, Pennington, NJ, 2000), p. 175.
[15] H. Windischmann and K. J. Gray, Diamond Relat. Mater. **4**, 1222 (1995).
[16] J. Michler, M. Mermoux, Y. von Kaenel, A. Haouni, G. Lucazeau, and E. Blank, Thin Solid Films **357**, 189 (1999).
[17] J. Yu, J. G. Kim, J. O. Chung, and D. H. Cho, J. Appl. Phys. **88**, 1688 (2000).
[18] R. C. Cammarata, T. M. Trimble, and D. J. Srolovitz, J. Mater. Res. **15**, 2468 (2000).
[19] J. Tersoff and F. K. LeGoues, Phys. Rev. Lett. **72**, 3570 (1994).
[20] A. Rajamani and B. W. Sheldon (unpublished).
[21] J. R. Morris, C. L. Fu, and K. M. Ho, Phys. Rev. B **54**, 132 (1996).
[22] O. A. Shenderova, D. W. Brenner, and L. H. Yang, Phys. Rev. B **60**, 7043 (1999).
[23] O. A. Shenderova and D. W. Brenner, Phys. Rev. B **60**, 7053 (1999).
[24] H. T. Johnson and L. B. Freund, J. Appl. Phys. **81**, 6081 (1997).
[25] S. C. Seel, C. V. Thompson, S. J. Hearne, and J. A. Floro, J. Appl. Phys. **88**, 7079 (2000).